

# Pion polarizabilities measurement at COMPASS

Guskov Alexey on behalf of the COMPASS collaboration

Joint Institute for Nuclear Research, Dzhelapov Laboratory of Nuclear Problems, Dubna, Russia

avg@nusun.jinr.ru

The electromagnetic structure of pions is probed in  $\pi^- + (A, Z) \rightarrow \pi^- + (A, Z) + \gamma$  Compton scattering in inverse kinematics (Primakoff reaction) and described by the electric ( $\overline{\alpha}_\pi$ ) and the magnetic ( $\overline{\beta}_\pi$ ) polarizabilities that depend on the rigidity of pion's internal structure as a composite particle. Values for pion polarizabilities can be extracted from the comparison of the differential cross section for scattering of pointlike pions with the measured cross section. The pion polarizability measurement was performed with a  $\pi^-$  beam of 190 GeV. The high beam intensity, the good spectrometer resolution, the high rate capability, the high acceptance and the possibility to use pion and muon beams, unique to the COMPASS experiment, provide the tools to measure precisely the pion polarizabilities in the Primakoff reaction. The preliminary result for pion polarizabilities under the assumption of  $\overline{\alpha}_\pi + \overline{\beta}_\pi = 0$  is  $\overline{\alpha}_\pi = -\overline{\beta}_\pi = (2.5 \pm 1.7_{stat.} \pm 0.6_{syst.}) \times 10^{-4} fm^3$ .

## 1 Introduction

Pion polarizabilities characterize the pion interacting as a complex  $q\bar{q}$  system with external electromagnetic fields. They are fundamental parameters of pion physics and the comparison of theoretically predicted and directly measured values provides a stringent test for various theoretical models. Among different models chiral perturbation theory ( $\chi PT$ ) is one of the most successful tools in describing low energy hadron properties and provides predictions for these two parameters [1]:  $\overline{\alpha}_\pi = 2.93 \pm 0.5 \times 10^{-4} fm^3$ ,  $\overline{\beta}_\pi = -2.77 \pm 0.5 \times 10^{-4} fm^3$ . The predictions of other theoretical models, like dispersion sum rules, QCD sum rule and quark confinement model lie in the range  $(2-8) \times 10^{-4} fm^3$  for the absolute values of  $\overline{\alpha}_\pi$  and  $\overline{\beta}_\pi$  (See [2],[3]). Several attempts were already done using different approaches to measure these quantities (See Tab. 1, [12]). The results obtained are affected by large uncertainties and there are large discrepancies between them and the  $\chi PT$  prediction. The new measurement performed with the COMPASS spectrometer will contribute to clarify the situation.

## 2 Primakoff reaction.

The Primakoff reaction  $\pi^- + (A, Z) \rightarrow \pi^- + (A, Z) + \gamma$  can be treated as Compton scattering of a virtual photon, provided by the nucleus, on the pion. The momentum transferred to the nucleus in a Primakoff reaction is very small ( $Q \ll m_\pi$ ).

Data	Reaction	$\bar{\alpha}_\pi$ [ $10^{-4} fm^3$ ]
Lebedev [4]	$\gamma + N \rightarrow \gamma + N + \pi$	$20 \pm 12$
PLUTO [5]	$\gamma\gamma \rightarrow \pi^+\pi^-$	$19.1 \pm 4.8 \pm 5.7$
DM1 [6]	$\gamma\gamma \rightarrow \pi^+\pi^-$	$17.2 \pm 4.6$
DM2 [7]	$\gamma\gamma \rightarrow \pi^+\pi^-$	$26.3 \pm 7.4$
Mark II [8]	$\gamma\gamma \rightarrow \pi^+\pi^-$	$2.2 \pm 1.6$
Serpukhov [9]	$\pi + Z \rightarrow \pi + Z + \gamma$	$6.8 \pm 1.4 \pm 1.2$
Data	Reaction	$(\bar{\alpha}_\pi + \bar{\beta}_\pi)$ [ $10^{-4} fm^3$ ]
Serpukhov [10]	$\pi + Z \rightarrow \pi + Z + \gamma$	$1.4 \pm 3.1 \pm 2.8$
Data	Reaction	$(\bar{\alpha}_\pi - \bar{\beta}_\pi)$ [ $10^{-4} fm^3$ ]
Mami A2 [11]	$\gamma + p \rightarrow \gamma + \pi^+ + n$	$11.6 \pm 1.5 \pm 3.0 \pm 0.5$

Table 1: Experimental values of  $\bar{\alpha}_\pi$ ,  $(\bar{\alpha}_\pi + \bar{\beta}_\pi)$ ,  $(\bar{\alpha}_\pi - \bar{\beta}_\pi)$

In the anti-laboratory system the differential cross section is described by the formula:

$$\frac{d^3\sigma}{dQd\omega_1d(\cos\theta)} = \frac{2\alpha^3 Z^2}{m_\pi^2 \omega_1} \frac{Q^2 - Q_0^2}{Q^4} |F_A(t)|^2 \cdot \left( F_{\pi\gamma}^{Pt} + \frac{m_\pi \omega_1^2}{\alpha} \cdot \frac{\bar{\alpha}_\pi(1 + \cos^2\theta) + 2\bar{\beta}_\pi \cos\theta}{(1 + \frac{\omega_1}{m_\pi}(1 - \cos\theta))^3} \right) \quad (1)$$

where  $Q_0^2 = (\frac{m_\pi \omega_1}{p_{beam}})^2$ ,  $m_\pi$  is the pion mass,  $\omega_1$  the energy of the virtual photon,  $\theta$  the angle between the real photon and the virtual photon directions and  $F_A(t)$  the electromagnetic form factor of the nucleus ( $F_A(t) \approx 1$  for  $Q \ll m_\pi/c$ ).

Here,  $F_{\pi\gamma}^{Pt}$  [13] describes the differential Compton cross section for the scattering of photons on a point-like spin-0 particles. The main characteristic of the cross section (Eq. (1)) is that it depends on  $(\bar{\alpha}_\pi + \bar{\beta}_\pi)$  at forward angles and on  $(\bar{\alpha}_\pi - \bar{\beta}_\pi)$  at backward angles.

### 3 Primakoff reaction studies at COMPASS.

The Primakoff reaction studies at COMPASS during the pilot hadron run in 2004 were performed with a 190 GeV  $\pi^-$  beam and Pb target. Additional samples with Cu, C and empty targets and a 190 GeV  $\mu^-$  beam were used to study background processes and estimate systematic errors. COMPASS provides unique conditions for the investigation of the Primakoff process: silicon detectors (spacial resolution better than  $16\mu m$ ) for the vertex position reconstruction and for the measurement of the pion scattering angle, an electromagnetic calorimeter for the photon 4-momentum reconstruction and a magnetic spectrometer for the determination of the scattered pion's momentum ([14],[15],[16],[18],[17]). Primakoff triggers were mainly based on the usage of the electromagnetic calorimeter and hodoscopes.

In our analysis we selected events with one primary vertex in the target region, one well measured outgoing track and one cluster in the central region of electromagnetic calorimeter. The exclusivity of Primakoff events is guaranteed by cuts on the total energy and  $Q^2$ . In addition to the electromagnetic scattering we have diffractive scattering processes with the same signature, for which the

momentum transfer is not zero. The diffractive scattering produces a significant background in the region of large  $Q^2$  while the peak at  $Q^2 = 0$  corresponds to the Primakoff events. The contribution of the pion diffractive scattering can be deduced from the comparison of the  $Q^2$ -distributions for pions and muons (see Fig. 1). In our analysis we use events with  $Q^2 < Q_{max}^2 = 6.5 \times 10^{-3} (GeV/c)^2$ . To take into account the background from diffractive scattering in the Primakoff sample, we fit it with an exponential function in the range  $(2 \times 10^{-2} - 1 \times 10^{-1}) (GeV/c)^2$  and extrapolate the fitted curve to  $Q^2 = 0$ . We also excluded the events with a  $\pi\gamma$  invariant mass  $M_{\pi\gamma} > 3.75 \times m_\pi$  to prevent misidentification of  $\rho^-$ -meson decay events due to the missing reconstruction of one of the photons from the  $\pi^0 \rightarrow \gamma\gamma$  decay as Primakoff events. Due to similar reasons we have some background from the decay of beam kaons ( $\sim 4\%$  in the beam)  $K^- \rightarrow \pi^- + \pi^0$ . It was estimated and subtracted using the data with beam kaon decays up- and downstream of the target. The contribution of kaon, so called empty target background, is shown in Fig. 2.

## 4 Primakoff scattering on different nuclear targets

The comparison of data samples collected with different targets provides the possibility to study the behavior of the signal/background ratio (ratio of the Primakoff signal versus the diffractive scattering background) for different materials and to check the  $Z^2$  dependence for the Primakoff cross section. In Fig. 3 are shown the  $Q^2$ -distributions for lead, copper and carbon. We observe that, compared to the other targets with smaller  $Z$ , the ratio of the Primakoff signal over the diffractive background is larger for lead. This confirms the goodness of our choice of lead as the main target material.

To check the  $Z^2$ -dependence we measured the total Primakoff cross sections for copper and carbon normalized by the measured cross section for lead  $\sigma/\sigma_{Pb}$ . The test for the  $Z^2$  dependence of the Primakoff cross section is presented in Fig. 4. We can observe that the measured values satisfy the  $Z^2$  dependence rule for a wide range of  $Z$ . This proves that our selection criteria effectively select Primakoff events and reject background events.

## 5 Pion polarizability extraction under the assumption of $\overline{\alpha}_\pi + \overline{\beta}_\pi = 0$

For a preliminary result on polarizabilities under assumption of  $\overline{\alpha}_\pi + \overline{\beta}_\pi = 0$  we compared the shapes of the differential cross sections  $d\sigma/d\omega$  measured and theoretically predicted for a point-like pion, where  $\omega = E_\gamma/E_{beam}$  is the relative energy of emitted photon. Only part of the total statistics for Pb target was used (about 7500 events in selected  $\omega$ -range). For the calculation of the acceptance we used a Monte Carlo simulation based on the Primakoff event generator POLARIS ([19]) and GEANT3 for the COMPASS setup description. The acceptance function (Fig. 5) has a smooth shape in the selected  $\omega$ -range and a similar behavior for pions and muons. That means that the COMPASS

geometry and selection criteria are convenient to study the Primakoff reaction and the muon events can be used as a reference. Since the simulation was based on the Born approximation for the cross section, radiative corrections for Compton vertex, multiple photon exchange, vacuum polarization and nuclear charge screening by electrons were taken into account. Fig. 6 shows the  $\omega$ -distributions for the measured signal, diffractive and empty target backgrounds. The ratio of the measured cross section to the prediction for a point-like particle is presented in Fig. 7 and 8 for pions and muons. In both cases it was fitted by a function of two free parameters: the absolute normalization and  $\overline{\beta_\pi}$ . In the case of muons the result of fit is consistent with the hypothesis of unstructured particles while for pions the preliminary result is  $\overline{\alpha_\pi} = -\overline{\beta_\pi} = 2.5 \pm 1.7 \times 10^{-4} fm^3$ . We estimated that the main contribution to the systematic uncertainty comes from the MC description and the total systematic uncertainty is  $\pm 0.6 \times 10^{-4} fm^3$ .

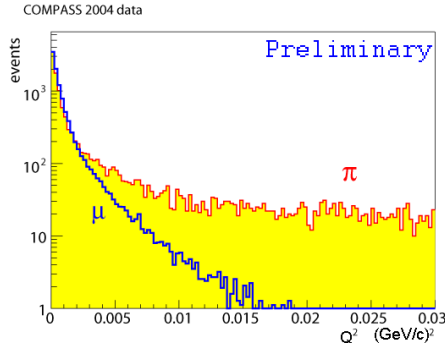


Figure 1:  $Q^2$ -distribution for pions and muons.

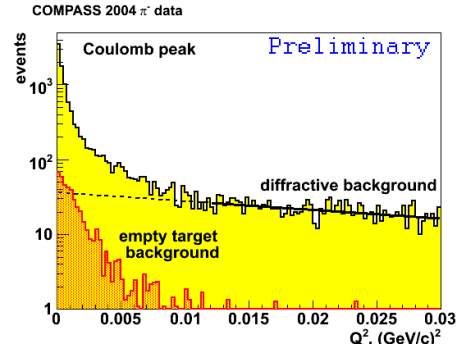


Figure 2:  $Q^2$ -distribution for 2+1 mm lead target. Diffractive and empty target backgrounds are shown.

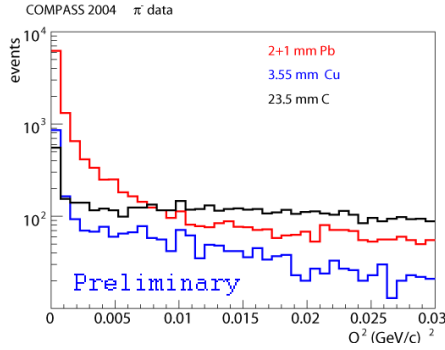


Figure 3:  $Q^2$  distributions for lead, copper and carbon targets.

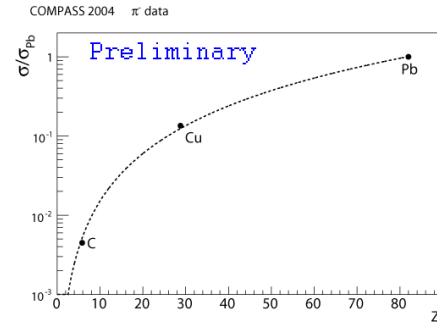


Figure 4:  $Z^2$ -dependency of Primakoff cross section.

## References

- [1] Gaser, Ivanov, Sainio NP B745 (2006) 84

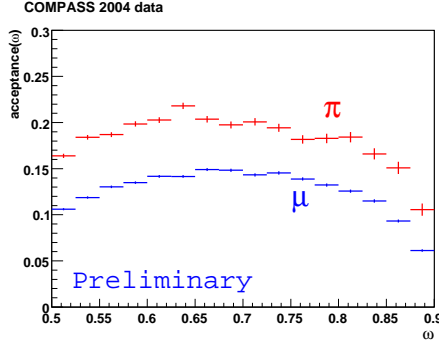


Figure 5: Acceptance for pions and muons as function of  $\omega$ .

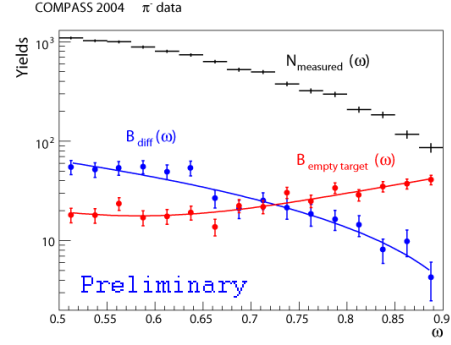


Figure 6:  $\omega$ -distributions for pions for measured signal, diffractive and kaon backgrounds.

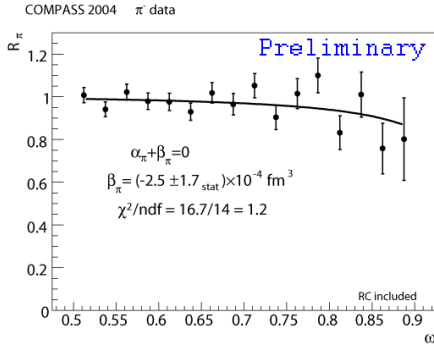


Figure 7: Ratio of Primakoff cross sections for pions as function of  $\omega$ .

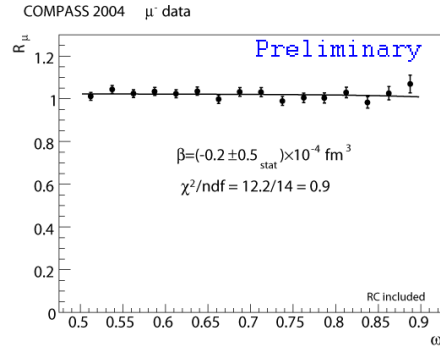


Figure 8: Ratio of Primakoff cross sections for muons as function of  $\omega$ .

- [2] J. Portoles, M.R. Pennington, *The second DaΦne Physics Handbook* v.2, 579 (1999), hep-ph/9407295
- [3] C.A. Wilmot, R.H. Lemmer, *Phys. Rev. C* **65**, 035206 (2002)
- [4] T.A. Aibergenov et al., *Czech J. Phys B* **36**, 948 (1986)
- [5] C. Berger et al., *Z. Phys.* **C26** 199 (1984)
- [6] A. Courau et al., *Nucl. Phys.* **B271** 1 (1986)
- [7] Z. Ajaltoni et al., *VII Int. workshop on photon-photon collision* Paris (1986)
- [8] J. Boyer et al., *Phys. Rev* **D42**, 1350 (1990), D. Babusci et al., *Phys Lett.* **B277**,158 (1992)
- [9] Yu M. Antipov et al., *Phys. Lett.* **B121**, 445 (1983)
- [10] Yu M. Antipov et al., *Z. Phys.* **C26**, 495 (1985)
- [11] J. Ahrens et al., *Eur. Phys. J* **A23** 113 (2005)

- [12] L.V. Fil'kov, V.L. Kashevarov Phys.Rev. **C73** 035210 (2006)
- [13] M. Buenerd, Nucl. Phys. **A361** 111 (1995)
- [14] F. Bradamante, S Paul et al., CERN Proposal COMPASS, <http://wwwcompass.cern.ch> , CERN/SPSLC 96-14, SPSC/P297; CERN/SPSLC 96-30, SPSC/P297, Addendum 1
- [15] P. Abbon , E. Albrecht et al., The Compass Experiment at CERN. NIMA 577 (2007) 455-518
- [16] M. A. Moinester et al., hep-ex/0301024
- [17] M. A. Moinester, Pion polarizabilities and Hybrid meson structure at COMPASS, hep-ex/0012063
- [18] A. Olchevski, M. Faessler, Experimental requirements for COMPASS Initial Primakoff Physics program, COMPASS coll. Meeting 2001.
- [19] M. Buenérd Prospects for hadron electromagnetic polarizability measurement by radiative scattering on a nuclear target, NIM A361 (1995) 111